

THE MECHANISM OF GRAIN GROWTH IN CERAMICS

by

C. M. Kapadia and M. H. Leipold
Research Assistant and Associate Professor
Department of Metallurgical Engineering and Materials Science
University of Kentucky
Lexington, Kentucky 40506

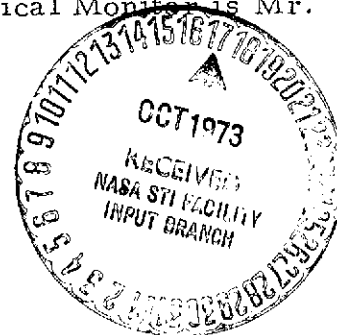
Abstract

The theory of grain boundary migration as a thermally activated process is reviewed, the basic mechanisms in ceramics being the same as in metals. However, porosity and non-stoichiometry in ceramic materials give an added dimension to the theory and make quantitative treatment of real systems rather complex. Grain growth is a result of several simultaneous (and sometimes interacting) processes; these are most easily discussed separately, but the overall rate depends on their interaction. Sufficient insight into the nature of rate controlling diffusion mechanisms is necessary before a qualitative understanding of boundary mobility can be developed.

Acknowledgment

Supported by Lewis Research Center of NASA Through Grant NGL-018-001-042, Cleveland, Ohio. Technical Monitor is Mr. W. Sanders.

Reproduced by
NATIONAL TECHNICAL
INFORMATION SERVICE
US Department of Commerce
Springfield, VA. 22151



(NASA-CR-135673) THE MECHANISM OF GRAIN
GROWTH IN CERAMICS (Kentucky Univ.)

52-p HC \$4.75

CSCL 11F

N73-32425

SI

Unclas
G3/17 15712

I. INTRODUCTION

Grain growth is an inherent phenomenon accompanying most fabrication processes in ceramics. The influence of grain size on behavior has been extensively studied¹⁻⁸ and the importance of grain size control cannot be over emphasized. Control is also needed to permit systematic evaluation of its influence on various properties. Here an understanding of the effect of microstructure (e.g. pore location, nature of grain boundary second phase) on grain growth is essential. The purpose of this paper is to present the current understanding of grain growth in ceramics by consolidating different features of boundary migration in relation to numerous material characteristics which influence it.

Initially, the basic thermodynamic driving force for grain growth is given, followed by a discussion of the fundamental equation for rate of grain boundary migration as an activated process. The details of the fundamental process are then modified to include the influence of the many material factors such as porosity and impurities. Each of these in turn is divided into a number of individual factors and appropriate theoretical and experimental concepts are introduced. Wherever possible, these concepts are illustrated by experimental observations in ceramics and metals. Differences in behavior between the two fields whenever they exist are noted. Since real ceramics seldom behave as predicted theoretically, or at least by simple theories, deviations in behavior are also mentioned.

Phenomena most commonly observed in ceramics like limiting grain size and discontinuous grain growth are also briefly discussed. Finally, a general expression for grain growth is developed describing the kinetics of grain growth from the knowledge of these rate controlling mechanisms in the system.

For convenience, the nomenclature in this review is defined below.

a	= lattice parameter at the grain boundary
C	= impurity atom fraction in the bulk
c	= concentration of the liquid phase at the grain boundary
D_ℓ	= diffusion coefficient of rate controlling species in the liquid
D_L	= limiting grain size
\bar{D}_o	= initial grain size
\bar{D}_t	= average linear intercept grain size at sintering time = t
D_o^i	= pre exponential for impurity diffusion at grain boundary
E	= strain energy term
F_b	= force on an atom situated on pore free boundary
F_b^B	= force acting on the pore free boundary
F_b^N	= force per unit area acting on the pore free boundary
h	= Planck's constant = 6.63×10^{-27} erg-sec.
K	= distribution coefficient $\approx 10^4$
M	= molecular weight of solid
m	= integer which determines the mechanism of pore transport
M_b	= mobility of the pore-free grain boundary
M_p	= intrinsic pore mobility
n	= grain growth exponent
N	= number of pores per atom at the grain boundary = ratio of pores to atoms at the boundary = N_p
N_a	= average number of pores per unit area of the boundary
N_t	= number of pores per boundary
N_v	= number of atoms per unit volume
P	= porosity of compact

Q_G	= activation energy (enthalpy) of grain boundary migration per mole
Q_i	= activation energy for impurity diffusion at the grain boundary
Q_p	= activation energy for pore migration
R	= gas constant = 1.98 cal/mole/degree
r	= average radius of curvature of the grain and is proportional to the average grain diameter \bar{D}_t
r_i	= radius of inclusion (pore or second phase particle)
r_n	= radius of second phase particle
r_p	= pore radius
S	= true solubility in gm/cm ³
S_{ss}	= solid-solid interface (grain boundary) area per unit volume (superscript refers to D for densification, G for grain boundary mobility and T for total)
S_T	= total interface area per unit volume = $S_{sv} + S_{ss}$
S_{sv}	= solid-vapor interface (surface) area per unit volume
V	= Velocity of the grain boundary moving with the pores
V_m	= molar volume
V_i	= volume fraction of inclusion of radius r_i
V_n	= volume fraction of the second phase particle
γ	= grain boundary surface tension
Ω	= volume of the diffusing atomic specie
ΔS_G	= molar entropy of grain boundary migration = difference in entropy between activated state and ground state
δ	= depth of boundary diffusion layer $\approx 10^{-6}$ cm.
ρ	= density of the solid
γ_ℓ	= energy of the solid-liquid interface
Δv	= difference in valence between impurity and the host atom.

II. Driving Force for Grain Growth

The driving energy (often called driving force), that moves the boundary toward its center of curvature resulting in grain growth, is the difference in the free energy of the material on the two sides of a grain boundary. Since the grain boundary area per unit volume of the material goes down as the grains grow, grain growth is accompanied by a decrease in the total grain boundary energy.

The decrease in the free energy per mole on crossing the curved grain boundary is given⁹ by the Gibbs-Thompson Equation as

$$\Delta F_m = \frac{A\gamma V_m}{r} \quad (1)$$

(A is a constant of the order of 1 to 3 and depends on the type of curvature (spherical or cylindrical) of the grain boundary). For MgO, $\gamma = 10^3$ ergs/cm² at 1300°C and for a grain size of 5 μ , $\Delta F_m \sim 10^{-2}$ cal/mole. This is much smaller than the driving force for strain induced recrystallization in metals (25-100 cal/mole). For a single atom or ion going across the curved boundary, the change in free energy is given by

$$\Delta F = \frac{A\gamma\Omega}{r} \quad (2)$$

from which it follows that the force on the individual atom responsible for causing it to jump is

$$F_b \propto \frac{\gamma\Omega}{ra} \propto \frac{\gamma\Omega}{\bar{D}_t a} \quad (3)$$

since r is proportional to \bar{D}_t which is valid if the grain size distribution remains unchanged during grain growth.

III. Basic Grain Growth Kinetics (Grain Boundary Velocity)

The principle features of grain growth in ceramics are generally found to be the same as in metals which have been extensively studied.¹⁰⁻¹⁵ From this, the basic expression for boundary velocity (G) can be represented as a product of the driving force and the intrinsic mobility and based on absolute reaction rate theory¹⁰ is given by

$$G = \frac{d\bar{D}_t}{dt} = \Delta F_m \times M_b \times \frac{1}{a} \quad (4)$$

where ΔF_m = driving force per mole (eqn. 1)

$$M_b = \text{boundary mobility}^{10} = \frac{a^2}{h} \exp\left(\frac{\Delta S_G}{R}\right) \exp\left(-\frac{Q_G}{RT}\right) \quad (5)$$

This may be simplified into the familiar expression

$$\frac{d\bar{D}_t}{dt} = \frac{K}{\bar{D}_t} \quad (6)$$

which upon integration yields

$$\bar{D}_t^2 - \bar{D}_o^2 = Kt \quad (7)$$

with

$$K = \frac{AV_m}{h} \gamma a \exp\left(\frac{\Delta S_G}{R}\right) \exp\left(-\frac{Q_G}{RT}\right) \quad (8)$$

Equation (6) was derived with the assumption that the grain size distribution and the grain boundary configuration are independent of the average grain size. Only then are the average grain size and the average boundary curvature directly proportional to each other. Equation (7) has been observed for grain growth in high purity metals^{16, 17} and in very dense oxides.¹⁸

When grain growth inhibiting effects are present, the growth law is empirically better represented¹⁹ by

$$\bar{D}_t^n - \bar{D}_o^n = Kt \quad (9)$$

or

$$\bar{D}_t^n = Kt \quad (10)$$

if $\bar{D}_t \gg \bar{D}_o$, where the observed grain growth exponent (n) is commonly greater than the theoretically predicted value of 2. The inhibiting effects often become more and more pronounced as annealing time increases.

Eventually the grains cease to grow and a limiting grain size is said to have been reached ($n = \infty$). Very often a single value of n , often $n = 3$, is reported for inhibited growth; this can be interpreted here as a transient behavior (over a limited range of annealing time) observed when inhibiting factors are just beginning to affect normal growth.

IV. Inhibited Grain Growth Kinetics

Since the grain growth exponent (n) commonly observed is greater than 2, it is important to describe factors which cause deviations from normal behavior ($n = 2$). These growth limiting factors have been extensively discussed for metals^{20, 21} and are summarized in Table I. Factors (2) and (3) are important only in special cases; and when they are applicable, they give a second order effect. They are not discussed further. In contrast, the material dependent factors are found in most situations and have a significant effect on growth kinetics. Porosity and impurities then as a major grain growth controlling factors will be treated next.

A. Effect of Porosity on Grain Growth.

Pores are an important microstructural feature of powder compacts. By the nature of development of pore morphology during the sintering process²⁸, the pores lie either on grain boundary intersections or are distributed along individual boundaries. The boundary and the pores move together in normal growth with a velocity (V) which is given²⁹ by

$$V = \frac{M_b F_b}{1 + N(M_b/M_p)} \quad (11)$$

where $F_b \propto \frac{\gamma\Omega}{D_b a}$ (see eqn. 3) and is the force on an atom on pore free boundary

$$M_b = f(T) \propto a^2 \exp\left(\frac{\Delta S_G}{R}\right) \exp\left(\frac{-Q_G}{RT}\right) \text{ and is the pore-free grain boundary mobility} \quad (5)$$

$$M_p = \frac{1}{r_p} \exp\left(\frac{-Q_p}{RT}\right) \text{ and is the intrinsic pore mobility}^{30} \quad (12)$$

Table I
Factors Which Control Boundary Migration Rates

(1) Material Dependent

- a) Inclusions - porosity and second phase particles effectively reduce driving force ΔF ^{9, 10}
- b) Grain boundary atmospheres - solute impurity drag reduces intrinsic boundary mobility²²⁻²⁵
- c) Discontinuous liquid phase at grain boundary $\left(1 < \frac{\gamma}{\gamma_L} < \sqrt{3}\right)$ - effect is either to reduce γ and/or increase diffusion paths for atoms jumping across boundary.

(2) Specimen Dependant

- a) Free Surface Effect for small specimens - grain boundaries perpendicular to the free surface have a cylindrical curvature rather than spherical²⁶.

$$\Delta F_{\text{cylindrical}} = 1/2 (\Delta F_{\text{spherical}})$$
- b) Preferred Orientation - Boundaries between grains of identical orientation move slowly due to decrease in γ or an increase in Q_G ^{9, 11, 27}.

(3) Grain Size Distribution

A disproportionately large number of fine grains will be preferentially eliminated during grain growth. Hence, $r \propto \bar{D}_t^d$, $d > 1$; and $d\bar{D}/dt$ will decrease more rapidly than given in Eqn. 6.

The pores are assumed to remain spherical. Constants m and Q depend on mechanism of pore transport in the material.³⁰ Since r_p varies³¹ with average grain diameter \bar{D}_t , it is dependent indirectly on temperature; hence, the dependence of pore mobility (M_p) on temperature may not be straight forward.

The influence of porosity on grain growth is further complicated by the fact that such porosity in the powder compact could be due to incomplete densification and consequently pore volume changes during grain growth. In other cases the pore volume is constant due to the presence of gaseous species existing as a result of contamination of initial powder.³² These gaseous impurities leave gas bubbles during densification and give rise to residual porosity or entrapped porosity,³³ a phenomenon very common in hot-pressed powder compacts.

The complex expression for velocity (V) of a boundary in presence of pores (Eqn. (11)) can be reduced to a more convenient form if limiting cases are considered, namely, boundary mobility controlling ($M_p \gg N M_b$) or pore mobility controlling ($M_p \ll N M_b$). In some special cases a mixed behavior is observed wherein in addition to pore controlled grain boundaries there are some regions of the specimen where boundaries move without pore interference, this behavior occurs during discontinuous or abnormal grain growth. These three cases are summarized in Table II and will be now discussed separately.

(1) Boundary Control.

When the annealing temperature is low and the pore radius is small we have grain growth controlled by boundary mobility. The grain boundary velocity (V) is given by

$$V = M_b F_b \quad (13)$$

In terms of material dependent parameters, using Equations (3) and (5) one gets

$$V \propto a \frac{\gamma \Omega}{\bar{D}_t} \exp \left(\frac{\Delta S_G}{R} \right) \exp \left(- \frac{Q_G}{RT} \right) \quad (14)$$

Table II

Factors Controlling Grain Boundary Mobility

Controlling Factors		
1. Boundary Mobility (Normal growth)	2. Pore Mobility (Normal growth)	3. Both (Discontinuous growth)
<u>Relative magnitudes of mobilities</u>		
a) $\frac{M_p}{N} \gg M_b$	$\frac{M_p}{N} \ll M_b$	$M_b \gg M_p (\approx 0)$
<u>Boundary velocity equation</u>		
b) $V = M_b F_b$	$V = \frac{M_p F_b}{N}$ (N = number of pores)	$V = M_b F_b$ for those grains whose diameter is much larger than the matrix grain diameter.
c) Boundary mobility controls (n = 2)	Pore mobility controls (n > 2)	Mixed control
<u>Conditions when behavior is present</u>		
d) Low temperature, therefore, M_b is small	High temperature (anneal time could be small), therefore M_b is large	High temperature
e) Low anneal time and small grain size, therefore r_p is small and M_p is large	Large anneal time (Temperature could be low) and large grain size, therefore r_p is large and M_p is small	

This is true when impurities do not have appreciable influence on boundary mobility. However, the discussion in Sec. IV-B indicates that impurities do affect boundary migration rates, in fact boundary mobility (M_b) is lowered by addition of solute impurities which according to Table II-1a favors boundary controlled grain growth. This is clearly seen in case of MgO (0.5% porosity) at 1300°C³⁴ where undoped material gives $n = 3$ (pore control) while addition of Fe⁺³ gives $n = 2$ (boundary control).

(2) Pore Control

When the pores are large and close together there is pore control provided pores remain on grain boundaries. The dragging effect of pores becomes pronounced at very short anneal times at high temperature as can be seen for MgO³⁵ at 1650°C corresponding to Table II-2d, whereas at a lower temperature of 1450°C pore inhibition occurs only after 1000 min. (See Table II-2e).

The grain boundary velocity under pore control is given by

$$\frac{d\bar{D}_t}{dt} \approx V = \frac{M_p F_b}{N} \quad (15)^*$$

which from equations (3) and (12) gives the general equation for porosity controlled grain growth rate as

$$\frac{d\bar{D}_t}{dt} \approx \frac{1}{N} \frac{\gamma \Omega}{\bar{D}_t a} \frac{1}{r_p^m} \exp\left(\frac{-Q_p}{RT}\right) \quad (16)$$

This can be expressed in terms of N , \bar{D} and r_p as

$$\frac{d\bar{D}_t}{dt} \propto \frac{1}{N \bar{D}_t r_p^m} \quad (17)$$

*It can be seen from equation (15) that grain boundary migration ceases when the grain size reaches a magnitude such that either $M_p \left(\propto 1/r_p^m \approx \frac{1}{\bar{D}_t^m} \right)$ or $F_b \left(\propto \frac{1}{\bar{D}_t} \right)$ or both become very small. Such a limiting grain size can be reached at shorter anneal times at high temperatures or at larger times at low temperatures.

where N and r_p are functions of \bar{D}_t , and m depends on mechanism of pore transport. To obtain the grain growth exponent, n , by integration of equation (17), the latter must be expressed in a convenient form like $\frac{d\bar{D}_t}{dt} \propto \frac{1}{\bar{D}_t^s}$ where s depends on value of m and the functional relationship of N and r_p with \bar{D}_t . These two dependencies will be discussed separately.

Dependence of N on \bar{D}_t . In the literature^{29, 36} N is normally defined as average number of pores per boundary. Since sweeping of pores along with the boundaries require pore coalescence,³¹ N cannot increase as \bar{D}_t increases. A convenient assumption often made is $N \approx \frac{1}{\bar{D}_t}$. However, since equation (11) is written in terms of M_b , the pore-free boundary mobility, it is related physically to the atom jump across the boundary. Thus, a more logical choice of units for F_b would be force per atom whereupon N is the number of pores per atom, equal to the ratio of pores to atoms at the boundary $\approx \frac{a^2}{f^2}$; where f = inter-pore spacing. For pores on the grain boundary, a reasonable assumption would be $f \approx \bar{D}_t$ in which case $N \approx \frac{1}{\bar{D}_t^2}$. An exact, and perhaps better, functional relationship of N on \bar{D}_t would require extensive quantitative microscopy of the annealed specimens used for grain growth studies.

Dependence of r_p on \bar{D}_t . For pores being dragged with the grain boundaries a linear relation is often assumed^{31, 36, 37} between r_p and \bar{D}_t ($r_p \approx \bar{D}_t$) for convenience although a closer examination suggests that the dependence may not be simple.³⁸

The grain growth exponent n can be determined if magnitude of integer m is known. Shewmon³⁹ has quantitatively shown that for spherical pores, m depends on mechanism of pore transport.

From equation (17) if we introduce the grain size dependence of N and r_p (namely, $N \approx \frac{1}{\bar{D}_t^2}$; $r_p \approx \bar{D}_t$) we obtain

$$\frac{d\bar{D}_t}{dt} \propto \frac{1}{N \bar{D}_t^m r_p^m} \approx \left(\frac{1}{\bar{D}_t^2} \right) \left(\frac{1}{\bar{D}_t} \right) \left(\bar{D}_t^m \right) \approx \frac{1}{\bar{D}_t^{m-1}} \quad (18)$$

which on integration gives $\bar{D}_t^m - \bar{D}_0^m = Kt$ (19)

which is of the same form as equation (9) with the value of grain growth exponent $n = m$. Due to uncertainty in dependence of N and r_p on \bar{D}_t , equations (18) and (19) are valid, limited by the assumptions described. Further since it is possible that more than one transport mechanism may be operating at the same time, experimental values of n may not correspond to any single theoretical prediction.

Brook³⁶ has given a treatment similar to above except that in equation (15) he has defined F_b as the force acting on the pore free boundary (which we shall denote by F_b^B) and N is the total number of pores per boundary. Henceforth, in order to distinguish the total number of pores per boundary from the number of pores per atom at the boundary, we denote the former as N_t and the latter by N_p . Since F_b^B in Brook's treatment is the pressure decrease across the boundary owing to its curvature $\left(= \frac{2\gamma}{\bar{D}_t} \right)$ multiplied by the area of the boundary ($\propto \bar{D}_t^2$) we have

$$F_b^B = \frac{2\gamma}{\bar{D}_t} \bar{D}_t^2 = 2\gamma \bar{D}_t \quad (20)$$

Hence, equation (15) reduces to

$$\frac{d\bar{D}_t}{dt} \propto \frac{\gamma \bar{D}_t}{N_t r_p^m} \propto \frac{\bar{D}_t}{N_t \bar{D}_t^m} \approx \frac{1}{N_t \bar{D}_t^{m-1}} \quad (21)$$

It can be seen that equation (21) reduces to equation (18) if N_t , the number of pores per boundary, is a constant,^{29,36} which will be true if the pores existed only at boundary intersections (grain corners). On other hand, if there are many pores distributed on individual boundaries,^{29,36}

$$N_t \approx \frac{1}{\bar{D}_t} \text{ and we would have } \frac{d\bar{D}_t}{dt} \propto \frac{1}{\bar{D}_t^{m-2}} \quad (22)$$

which upon integration gives

$$\bar{D}_t^{m-1} - \bar{D}_0^{m-1} = Kt \quad (23)$$

In contrast Nichols²⁹ has defined F_b differently (the force per unit area acting on the pore free boundary, denoted by F_b^N .) In this case, N will be average number of pores per unit area of the boundary, equal to N_a . If $F_b^N \propto \frac{1}{\bar{D}_t}$, equation (15) reduces to

$$\frac{d\bar{D}_t}{dt} \propto \frac{1}{N_a \bar{D}_t r_p^m} \approx \frac{1}{N_a \bar{D}_t \bar{D}_t^m} \approx \frac{1}{N_a \bar{D}_t^{m+1}} \quad (24)^\dagger$$

For pores lying only at the grain corners ($N_t = \text{constant}$), we have $N_a^* \approx \frac{N_t}{\bar{D}_t^2} \propto \frac{1}{\bar{D}_t^2}$ and equation (24) reduces to $\frac{d\bar{D}_t}{dt} \propto \frac{1}{\bar{D}_t^{m-1}}$ which is of the same form as equation (18) and on integration gives

$$\bar{D}_t^m - \bar{D}_o^m = Kt \quad (19)$$

If pores are on individual grain boundaries, $N_a \propto \frac{1}{\bar{D}_t^3}$ and equation (24) gives $\frac{d\bar{D}_t}{dt} \propto \frac{1}{\bar{D}_t^{m-2}}$ and $\bar{D}_t^{m-1} - \bar{D}_o^{m-1} = Kt$ which are the same form as equations (22) and (23) above.

We conclude that depending on mode of pore transport (i. e. the value of integer (m) and based on the assumption that $r_p \approx \bar{D}_t$ we get essentially two sets of grain growth exponent (n) namely, $n = m$ for pores at boundary intersections and $n = m - 1$ for pores on individual grain boundaries. The values of n for both the cases of pore location are given in Table III for each mechanism of pore transport. Although one normally expects values of $n > 2$ for porosity controlled grain growth, there are certain pore transport mechanisms wherein $n \leq 2$ is predicted.

[†] $\exp\left(-\frac{Q_p}{RT}\right)$ although present in equations (17), (21) and (24) is omitted for brevity.

* In the original work, Nichols²⁹ has incorrectly taken N_a in equation (24) as average number of pores per boundary rather than number of pores per unit area of the grain boundary; this gives a different dependence of $\frac{d\bar{D}_t}{dt}$ on \bar{D}_t and increases the grain growth exponents in equations (19) and (23) by 2.

Table III

Values of m for Different Pore Transport Mechanisms and Corresponding Grain Growth Exponents(n)

Mechanism	m	n		Conditions when applicable		
		$n = m^{\dagger}$ (pores at boundary intersection)	$n = m - 1^*$ (pores on individual grain boundaries)	Pore radius r_p	Temperature	Vapor Pressure
Surface diffusion	4	4	3	small	low	low
Volume diffusion	3	3	2	Intermediate	Intermediate	low
Vapor transport (p = constant)	3	3	2	Large ($\geq 1\mu$)	high	high
Vapor transport $\left(p = \frac{2\gamma_{sv}}{r_p}\right)$	2	2	1	Large ($\geq 1\mu$)	high	high

† For $N_p \approx \frac{1}{\bar{D}_t^2}$ in Eqn (18); $N_t = \text{const.}$ in Eqn. (21); $N_a \approx \frac{1}{\bar{D}_t^2}$ in Eqn. (24).

* For $N_t \approx \frac{1}{\bar{D}_t}$ in Eqn. (21); $N_a \approx \frac{1}{\bar{D}_t^3}$ in Eqn. (24)

Bannister obtained $n = 2$ in 98% dense BeO ⁴⁰ while for F^- doped MgO ⁴¹ a value of n as low as unity has been observed. It is often observed in photomicrographs of ceramic materials that pores actually lie both on grain boundaries and at grain corners and hence the above two cases of pore location by themselves may be somewhat idealized. In practice one could observe a behavior intermediate between these two cases.

To better understand the discussion of pore control, a comparison is made with available experimental grain growth data. There is a growing evidence^{35, 37} that pores subjected to a force such as the pull of a grain boundary can move through the solid by vapor transport or surface diffusion depending on temperature and pore size. For UO_2 , MacEwan⁴² observed values of n between 2.5 and 3 while for Al_2O_3 , Coble⁴³ obtained $n = 3$. These correspond to pore migration either by vapor transport (pressure = constant) or by volume diffusion. However, the activation energies in both cases approximately agree³⁷ with the heat of vaporization of the diffusing specie responsible for pore transport, suggesting vapor transport of pores as the controlling mechanism.

In contrast, low temperature pore migration in MgO ³⁵ ($n = 2$) is explained by surface diffusion but the pore structure is continuous (See Section IV-A-5) rather than discontinuous. At higher temperatures lattice diffusion and vapor transport with discontinuous pores become increasingly important and $n = 3$ as expected. White, et al.⁴⁴ observed $n = 5$ for grain growth in MgO in presence of water vapor up to 1000°C and $n = 4$ at higher temperatures. From Table III, the most likely mechanism of pore movement in this case is again by surface diffusion.

(3) Limiting Grain Size, D_L .

In the previous section it was seen that movement of a grain boundary is hindered whenever it intersects a pore giving the grain growth exponent n greater than 2. An extreme case of pore inhibition is wherein the boundary has trapped enough inclusions such that the surface tension force is unable (due to lack of sufficient curvature) to overcome the restraining force of the pores and grain growth in the

material ceases. Limiting grain size is said to have been reached; a situation present in most porous compacts. To conclude porosity inhibited grain growth, limiting grain size is treated in some detail in this section. Since second phase particles behave like pores at least as far as grain growth inhibition goes, this discussion can be generalized for any type of inclusions in the material, either pore or second phase particle. This, of course, does not consider the permanence of the inclusion in that pores may be removed by further densification.

The limiting grain size (D_L) is reached at short anneal times at high temperatures due to higher growth rates, while at low temperatures, very long anneal times are required to give limited growth. Assuming a spherical shape for the inclusion with uniform distribution in the matrix, it can be shown^{9, 26} that:

$$D_L \approx 1.3 \frac{r_i}{V_f} \quad (25)$$

As one usually finds a distribution of inclusion sizes rather than a single value, equation (25) should be written in the form

$$D_L \approx 1.3 \sum_j \frac{r_{ij}}{V_{fj}} \quad (26)$$

(V_{fj} is the volume fraction of inclusions with radius r_{ij}). Under these conditions, the rate of growth will be controlled not by the average grain size present (\bar{D}), but by difference between this grain size and the limiting one, (D_L), so that the boundary migration rate is given by

$$\frac{d\bar{D}_t}{dt} = K \left(\frac{1}{\bar{D}_t} - \frac{1}{D_L} \right) \quad (27)$$

where K is defined in equation (8). Equation (27) on integration gives

$$\frac{D_o - \bar{D}_t}{D_L} + \frac{D_L - D_c}{D_L - \bar{D}_t} = \frac{K}{D_L^2} t. \quad (28)$$

Burke¹¹ applied equation (28) to correlate growth data for alpha-brass specimens containing a stable array of inclusions and found the agreement satisfactory.

The effectiveness of such inclusions in retarding grain growth is expected to depend on boundary-inclusion surface energy and on their location. Wollfrey⁴⁵ has taken into account the geometrical location of the inclusion by modifying equation (25) (applicable only for uniform distribution of inclusions). A comparison of the effectiveness of inclusions as grain size stabilizers as a function of their location in the matrix is given Table IV. Limiting grain sizes are calculated for three different volume concentrations ($V_f = 0.1\%$, 1% , 10%) of inclusions of radii 0.5μ and 5μ . To aid comparison, the relative magnitudes of D_L for each location of inclusion are given below (numerical subscript to (D_L) refers to inclusion location):

$$V_f = 0.1\% \quad ; \quad (D_L)_1 = 4 (D_L)_2 = 40 (D_L)_3 = 100 (D_L)_4$$

$$V_f = 1\% \quad ; \quad (D_L)_1 = 4 (D_L)_2 = 15 (D_L)_3 = 20 (D_L)_4$$

$$V_f = 10\% \quad ; \quad (D_L)_1 = 4 (D_L)_2 = 4 (D_L)_3 = 4 (D_L)_4$$

Based on these comparisons, some general observations can be made:

- 1) Inclusions located on 3 grain edges are most effective in restraining boundary migration, while those randomly distributed are least effective. This effect was seen earlier in Table III for the case of pore controlled boundary migration wherein a comparison of columns 3 and 4 show that n values for pores at three grain intersections are greater than those for pores on individual grain boundaries; a larger n value corresponding to greater restraining effect of pores.
- 2) Very small quantities of inclusions are sufficient to stabilize grain size. This is in accordance with observation of $n > 2$ even for quite dense and high purity oxide³⁴ compacts.
- 3) The restraining effect of inclusions is more sensitive to their location when volume fraction of inclusion is small.
- 4) For inclusions in form of pores, a value of $V_f = 10\%$

Table IV

Limiting Grain Size, D_L (in microns) for Different Inclusion Locations

Location of inclusions	$(D_L) = f(r_i, V_f)$	Inclusion radius	$V_f = 0.1\%$	$V_f = 1\%$	$V_f = 10\%$
1. Random dispersion with inhibition by particles on 3 grain edges	$(D_L)_1 = 1.05 \frac{r_i}{V_f}$	$r_i = 0.5\mu$	525	52.5	5.25
		$r_i = 5\mu$	5250	525	52.5
2. Random dispersion with inhibition by particles at grain boundaries	$(D_L)_2 = 0.3 \frac{r_i}{V_f}$	$r_i = 0.5\mu$	150	15	1.5
		$r_i = 5\mu$	1500	150	15
3. Dispersed on grain boundaries only	$(D_L)_3 = 0.77 \frac{r_i}{V_f^{1/2}}$	$r_i = 0.5\mu$	12.2	3.85	1.22
		$r_i = 5\mu$	122	38.5	12.2
4. Dispersed at 3 grain edges only	$(D_L)_4 = 1.23 \frac{r_i}{V_f^{1/3}}$	$r_i = 0.5\mu$	6.15	2.82	1.32
		$r_i = 5\mu$	61.5	28.2	13.2

would correspond to interconnected porosity (pores entirely on grain boundaries) and the above comparison is probably not meaningful.

(4) Discontinuous Grain Growth

When grain boundary mobility is limited by pore mobility, the inherent boundary mobility is, of course, greater. In some instances, the boundary will be able to migrate past pores (pore separation) and trap them inside the grain. These large grains initially grow at a rate proportional to number of their sides.* When their diameter is much larger than the average matrix diameter, $D_g \gg \bar{D}_m$ the growth rate will be proportional to $\frac{1}{\bar{D}_m}$. Such localized uninhibited growth ($n = 2$) in spite of the presence of pores in the fine-grained matrix is often called discontinuous or abnormal grain growth. Such an abnormal growth has been observed for MgO ^{46, 47} of very high purity at temperatures high enough for some of the boundaries with high mobility to separate from pores. It is shown by Burke⁴⁹ that for a given value of r_p and matrix grain size \bar{D}_m , either an increase in M_p or a decrease in M_b will tend to inhibit pore breakaway and hence prevent discontinuous growth. In other words, this suggests that the ratio of M_b/M_p should be decreased to inhibit separation. Of the possibilities for decreasing this ratio, reduction in M_b is easier to accomplish and hence justifies further discussion.

A decrease in boundary mobility (M_b) can be achieved by impurities segregated at the grain boundaries either as second phase inclusions⁵⁴ (Section IV-B-1) or in solid solution (Section IV-B-2) as impurity atmosphere²⁵ giving a drag on the boundaries. There is also another way^{31b} in which soluble impurities affect M_b . They reduce both the surface tension of grain boundary (γ) and the energy of boundary-

* Von Neumann⁴⁸ has shown that the growth force is proportional to $(L-6)$, where L is the number of sides on a grain.

pore interface (γ_{sv}) giving a lower value of the equilibrium dihedral angle θ at the pore-grain boundary intersection ($\cos \frac{\theta}{2} = \frac{\gamma}{2\gamma_{sv}}$). A small value of θ will give a greater resistance to boundaries breaking away from pores, because for a given value of porosity, the fraction of boundary intercepted by pores is greater. Thus, a lower value of θ will, for the same porosity, tend to prevent discontinuous grain growth. Such an influence may well be the major cause of the utility of MgO as a sintering additive in Al_2O_3 . Several examples exist wherein impurities have been added to a matrix to prevent discontinuous grain growth, for instance $Al_2O_3 + MgO$ ^{25, 28, 50, 51} and $Y_2O_3 + ThO_2$ ⁵². Brook⁵³ has quantitatively shown that impurity additions can shift the onset of abnormal growth to a larger grain size. His explanation of the effect of sintering additives⁵⁴ is their delay of abnormal growth (pore-separation) beyond the grain size at which final densification is achieved.

(5) Grain Growth in Presence of Interconnected Porosity

Previous sections dealt mainly with boundary migration rates in the presence of small amounts of porosity. This section deals with grain growth in presence of larger porosity levels (> 5%) normally found during intermediate stage of sintering.

Pore controlled grain growth in presence of interconnected porosity (> 5%) differs from that in the final stage of sintering in that the rate is controlled by the rate of pore removal rather than migration of individual pores along with the grain boundary. It is postulated on basis of studies on oxides^{42, 55, 56} that the pore-removal and grain growth are caused by identical mechanisms of material transport. During intermediate stage sintering two distinct but simultaneous processes are involved.

- (a) Firstly, densification occurs, wherein the internal surface area (S_{sv}) decreases accompanied by new grain boundary area (S_{ss}). The driving force is a net reduction in the total interface energy (surface energy is approximately

three times grain boundary energy). According to Coble²⁸ the pore-boundary geometry during the intermediate stage of sintering approximates a continuous pore channel at three grain edges and maintains an essentially constant shape until the final stage begins. For sintering by volume diffusion, there is a vacancy diffusion flux from the cylindrical pores to boundaries between the grains. Since these diffusion paths through the grain volume will be shorter for smaller grain diameters, the rate of pore removal will be proportional to $\frac{1}{\bar{D}_t}$, i.e.

$$-\frac{dP}{dt} \propto \frac{1}{\bar{D}_t} \quad (29)$$

- (b) Secondly, grain growth occurs with a decrease in grain boundary area brought about by migration of solid-solid interfaces. The driving force here is the free energy difference of an atom across a curved interface.

With interconnecting porosity, increase in \bar{D}_t is accompanied by a decrease in the total interface area ($\bar{D}_t \propto \frac{1}{S_T}$) and $S_T = S_{ss}^T + S_{sv}$ since the total interface area consists not only of solid-solid interface but also solid-vapor interfaces. A decrease in solid-vapor interface during densification will create new solid-solid interface and hence

$$(\Delta S_{sv} = -\Delta S_{ss}^D) \quad (30)$$

The total change in solid-solid interface (ΔS_{ss}^T) results from two contributions, one an increase as a result of densification (ΔS_{ss}^D is positive) and one a decrease as a result of grain boundary mobility (ΔS_{ss}^G is negative) and is given by

$$\Delta S_{ss}^T = \Delta S_{ss}^D + \Delta S_{ss}^G \quad (31)$$

The change in grain size, however, is related to the change in total interfacial area (ΔS_T) which is given by

$$\Delta S_T = \Delta S_{ss}^T + \Delta S_{sv} \quad (32)$$

Substituting Eqn. (30) and (31) into (32) yields

$$\begin{aligned}\Delta S_T &= \Delta S_{ss}^D + \Delta S_{ss}^G - \Delta S_{ss}^D \\ &= \Delta S_{ss}^G\end{aligned}\quad (33)$$

It may thus be concluded for grain growth during interconnected porosity that:

- (1) Decrease in total interface area (S_T) equals decrease in solid-solid interface area (S_{ss}^G) by boundary migration.
- (2) From equation (31), net solid-solid interface (grain boundary) area (S_{ss}^T) can increase, decrease or remain constant during grain growth depending on relative rates of densification and boundary migration. Grain growth in presence of interconnected porosity is unusual since increase in grain size is normally associated with only a decrease in grain boundary area (S_{ss}).
- (3) As the solid vapor interface does not contribute directly to a decrease of S_T , grain growth can only occur after creation of new solid-solid interfaces. Therefore, the rate of growth is limited by the rate of pore removal (ΔS_{sv}).

The last conclusion is consistent with experiments wherein a linear relation, independent of temperature, has been observed between \bar{D}_t and relative density for porosity 5-20% in systems ZnO ⁵⁷, BeO ⁵⁸, Al_2O_3 ⁴³, Cu ⁵⁹ and Ag ⁶⁰. It is the basis for the equation

$$\frac{d\bar{D}_t}{dt} \propto - \frac{dP}{dt} \propto \frac{1}{\bar{D}_t} \quad (33)$$

On integration one gets $\bar{D}_t^n - \bar{D}_o^n = Kt$ with $n = 2$ which is observed for porous (density < 95%) BeO ⁴⁰, MgO ^{46, 61, 62}, CaO ⁶¹, NiO ⁶³ and UO_2 ⁶⁴. However, other work on oxide systems in the porosity range (7-40%) showed some disagreement. For BeO , Clare⁵⁸ obtained $n = 3$, while Felten⁶⁵ obtained $n = 1$. The explanation for latter behavior was given as the presence of a duplex structure, the secondary grain growth being rate determining in the intermediate stage. Values of $n = 2.5$ and 3 have been reported⁶⁶ for UO_2 and the discrepancy is explained as due

to extrinsic effects. For Mn-Zn ferrite in the intermediate stage^{67b}, $n = 2.3$ and increases to 3.8 on densification to the discontinuous porosity stage. For Ni ferrite,^{67c} n decreases with increasing temperature from 5 to 2.5 and is proposed to result from two processes acting simultaneously: (1) the formation of the Ni ferrite and (2) the growth of the Ni ferrite grains. On the other hand, n increases^{67a} monotonically from 2.5 to 3 with increasing temperature for $\text{Ca}_{0.16}\text{Zr}_{0.84}\text{O}_{1.84}$; a possible explanation being the interconnected pores are filled up by liquid phase at the grain boundaries (evident from photomicrographs) at higher temperatures. dD_t/dt would then be controlled by diffusion through the liquid phase giving $n = 3$ (Sec. IV-B-4) rather than by simultaneous pore removal. Disagreements were also observed in Al_2O_3 ⁴³, W_2O_6 ⁶⁸ and ZnO ^{57, 69} where $n = 3$, instead of 2 as predicted by equation (33).

Summarizing, the grain growth exponent most commonly observed in region of interconnected porosity is 2 and rate of grain growth depends on the rate of pore removal (densification). The enhancement of grain growth in presence of certain impurities can be explained by the ability of the latter to promote densification. Previous results also indicate that the linear relationship between grain size and density is temperature independent and gives the same activation energies for densification as for grain growth. Further, activation energy is that for the lattice diffusion of the cation,^{40, 42, 43, 57, 62} as confirmed by tracer diffusion studies. Table V gives a compilation of grain growth data for oxides in presence of interconnected porosity. Wherever possible, activation energies for grain growth and densification are compared with those for bulk diffusion of the cation obtained from self-diffusion studies. There is a considerable scatter in activation energies for each oxide especially for UO_2 wherein the energies are extremely sensitive to degree of hyperstoichiometry ($\frac{\text{O}}{\text{U}}$ ratio) and hence furnace atmosphere. There is however, some correspondence between activation energies for grain growth and cation self diffusion for cases where $n \approx 2$. Hence, for normal grain growth in presence of interconnected porosity the rate controlling mechanism is pore removal by lattice diffusion of the cation.

Table V

Sintering Data for Typical Oxides in Presence of Interconnected Porosity

Material	Investigator	Temp. °C	Sintering Atmos.	Grain Growth Exp. n	Activation Energies in Kcal per mole*		
					Q_D	Q_G	Q_L (Literature Value)
BeO	Bannister ⁴⁰	1500-1700	Vac	2.2	116±10	114	92(E) [†] (1550-1750°C) ^{70a}
	Clare ⁵⁸	1300-1500	N ₂ [†]	3	138	104	62.5(E) (1150-1800°C) ^{70b}
	Felton ⁶⁵	1700	H ₂	1			
CaO	Daniels, et al. ⁶¹	1300-1600	Air	2		110	81 (I) (1000-1600°C) ^{70e} 34 (E) (1000-1400°C) ^{70f}
MgO	Gupta ⁶²	1450-1600	Air	2	102±15	75.5	79 (I) (1400-1600°C) ^{70d}
	Daniels et al. ⁶¹	1450-1650	Air	2		60	
NiO	Y. Iida ⁶³	1500-1700	Ar, O ₂	2		55	46 (E) ^{70h} 56 (E) ⁷⁰ⁱ
ZnO	Gupta and Coble ⁵⁷	900-1050	Air	3	66±3 61±5	61±10	70-74(I) (850-1100°C) ^{70g}
	Nicholson ⁶⁹	900-1100	Dry O ₂	3		97.7	
Al ₂ O ₃	Coble ⁴³	1450-1600	Air	3	150	153±15	114±15 (I) (1650-1850°C) ^{70c}
Al ₂ O ₃ + 0.1 wt% MgO	Bruch ⁵¹	1600-1900	Dry H ₂	3	150	154	

Table V (Contd.)

UO ₂	Amato, et al. ⁶⁴	1450-1650	H ₂	2		115±8	110 (I) (1200-1600°C) ^{70j}
	Belle ^{66a}	1500-1700	H ₂	~1.6		59	88 (E) (1400-1700°C) ^{70l}
	Stehle ^{66d}	1550-1660		2		58	
	MacEwan ⁴²	1555-2440	{Ar, } Vac.}	2.5		87	73 (E) (1900-2150°C) ^{70k}
	Ross and Whitton ^{66c}	1155-1655	H ₂	2.5		75±5	
	Amato, et al. ^{66b}	1200-1400	steam CO ₂	2.2 2.5		49±7 46±6	85 (E) (1275-1650°C) ^{70m}
	Stehle ^{66d}	1550-1660		3.7		87	
	Amato, et al. ⁶⁴	1450-1630	H ₂	3		151±3	
	Hausner ^{66e}	1900-2600	Ar-He	~5.7		65	
WO ₃	Aitken ⁶⁸	900-1000	Air	3			
Ca _x Zr _{1-x} O _{2-x} (x = .16)	Tien and Subbarao ^{67a}	1600-2000	O ₂	2.5		80	109 (Ca ²⁺ , Zr ⁴⁺) ⁷⁰ⁿ

* Q_D, Q_G = Activation energies for densification and grain growth respectively, in the presence of continuous porosity; Q_L = activation energy from self diffusion studies for lattice diffusion of the cation in its own oxide in the specified temperature range.

† Symbols E and I denote activation energies for extrinsic and intrinsic behavior respectively.

† <100 PPM H₂O VAPOR

6. Summary of Grain Growth in Presence of Porosity

Grain growth is thus controlled by pore-grain boundary interactions as function of pore radius (r_p) and grain size (\bar{D}_t) and may be related by $\bar{D}_t = (\text{const}) (r_p)^\lambda$ where λ is some exponent depending on pore location and mechanism of pore transport. It has been shown⁵³ that for a particular case of pore transport by surface diffusion, a value of $\lambda > 2$ gives uninhibited grain growth while $\lambda < 1$ gives porosity controlled growth. For grain growth in porous compacts, the common sequence of pore-boundary interaction is that with increasing 1) anneal time, 2) pore radius and 3) average grain size, grain growth is first under boundary control ($\frac{M_p}{N} > \frac{M_b}{N}$), then pore control ($\frac{M_p}{N} < \frac{M_b}{N}$) and finally pore separation (discontinuous grain growth). Pore controlled boundary migration starts at shorter anneal times for high temperature than for low temperature. Also in porous materials, impurities in solid solution have three important effects: (1) they delay the onset of pore-controlled boundary migration i.e. $n = 2$ is observed for longer anneal times,⁵³ (2) they reduce^{31b} the dihedral angle (θ) at pore boundary intersection; that is, a pore with a small θ will have less tendency to migrate with the boundary and act as a greater drag on boundary migration as long as the boundary curvature is so small that the boundary cannot break away, (3) they give impurity drag²²⁻²⁴ on the moving boundary (Eqn. 37), thus preventing pore-boundary separation (discontinuous grain growth). Finally, it must be pointed out that due to a lack of detailed information about r_p dependence on \bar{D}_t (which needs knowledge of mechanism of pore motion) and the exact interaction between impurities and the matrix, a quantitative treatment of the growth process (boundary control vs. pore control) is not yet practical. The fundamental process controlling pore mobility may be altered in a particular system by other factors, e.g. the diffusion coefficients altered by the defect chemistry or by a different growth controlling mechanism such as second phase. Hence, the impurities may influence the pore

mobility (M_p) and boundary mobility (M_b) and this effect is treated next.

B. Effect of Impurities

Most ceramic fabrication processes involve compaction of fine powders. In general, cation impurities are inherent in the powder while anion impurities result from surface contamination of active initial powder, or trace impurities introduced in the material from wet preparation techniques³² (Cl^- , OH^-). In wrought metals, zone refining techniques can reduce the impurity level to less than 10 ppm. Such techniques are often not feasible for refractory materials and hence impurity content can be reduced only by proper handling and selected preparation techniques. It has been shown^{47, 71} that even minute amounts of foreign ions can greatly affect grain growth in oxide ceramics. Hence caution must be taken in the interpretation of grain growth kinetics in the so-called pure oxides (impurity level 200 ppm). Impurity controlled grain growth usually gives a value of $n = 3$ for the grain growth exponent.³⁶ However, the mechanisms that control the grain growth rate depend on the form in which these impurities exist in the material and these will be discussed next.

1. Impurity Precipitates

To observe grain growth in the presence of rate controlling precipitates, their coalescence is required. Coalescence of such second phase¹³ by lattice diffusion⁷² will control the boundary velocity and takes the form

$$\frac{d\bar{D}_t}{dt} = A \Omega \gamma a \left(\frac{1}{\bar{D}_t} - \frac{1}{D_L} \right) \exp \frac{\Delta S_G}{R} \exp \frac{-Q_G}{RT} \quad (34)$$

$$\text{where } D_L \approx \frac{r_n}{V_n} \quad (35)$$

assuming uniform distribution of inclusions in the matrix.

The growth of second phase particles is directly related to the surface tension at the interface between the matrix and the particles.

Because of the boundary-surface energy, the free energy per atom in a large particle is lower than in a small particle. This free energy difference is the driving force that causes the dissolution of small particles and the growth of large ones by the process of lattice diffusion. If \bar{r}_n = average radius of the second phase particles, those with $r_n > \bar{r}_n$ will tend to grow, the time dependence being⁷³

$$r_n \approx t^{\frac{1}{3}} \quad (36)$$

From Eqn. (35) this gives $D_L \approx t^{\frac{1}{3}}$ since volume fraction of second phase is expected to remain unchanged. Hence, the situation in presence of second phase inclusions can be described as follows:

when $\bar{D}_t \ll D_L$, inclusions have no effect on grain growth ($n = 2$)

when $\bar{D}_t > D_L$, inclusion-boundary separation has occurred

when $\bar{D}_t \approx D_L \approx t^{\frac{1}{3}}$, inhibited growth with $n = 3$, the activation energy being that for lattice diffusion of rate controlling specie.

Such a behavior is typical of metallic systems^{11, 74, 75} and is expected to control grain growth even in ceramic systems⁵⁴ when porosity effects are not dominant.

2. Solid Solution Impurities (isovalent)

A rather straight forward situation of solid solution is considered here wherein the impurity atom has identical valence as that of the host atom, giving no defect structure and the concentration of solute does not exceed the solubility limit so that strictly a single phase exists. Also, segregation of impurities or solid solution dopants at grain boundaries is expected from thermodynamic consideration based on Gibbs adsorption theory⁷⁶ which generally leads to conclusion that a monolayer of impurities are adsorbed on grain boundaries. However, hardness measurements,⁷⁷ autoradiography^{77a} and microprobe studies⁷⁸ generally lead to the conclusion that the affected layer may be at least hundreds of Angstroms; based on studies of grain boundary diffusion in MgO ,⁷⁹

solute atmospheres at grain boundaries are of order of $1\ \mu\text{m}$.

The mobility of a pore-free grain boundary (M_b) is given by²²

$$= \frac{\bar{D}_o^i}{RT} \left(\frac{1}{1 + 4N_v \delta K Ca^2} \right) \exp - \left(\frac{Q_G}{RT} \right); Q_G = Q_i + E \quad (37)$$

In absence of a defect structure and when impurity concentration is below the solubility limit, E is the interaction potential between the impurity atom and the grain boundary and is also known as the strain energy term. Zener⁸⁰ derived the expression for the strain energy,

$$E = 8\pi\mu R_h (\delta R)^2$$

where R_h is radius of the host ion, δR is the difference in the radii of the host (solvent) and the impurity (solute) ion, and μ is the shear modulus. For Al_2O_3 , the values of strain energies are 3.57, 6.49, and 5.26 K cal/mole for dissolved Cr^{3+} , Ti^{3+} , and Fe^{3+} respectively,

The above expression is a limiting case for low grain boundary driving force and high impurity content.

For large impurity concentrations and small grain size, Brook⁸¹ has shown that grain boundary velocity is given by $\frac{d\bar{D}_t}{dt} \propto \frac{1}{\bar{D}_t^2}$ where solubility of the impurity in the bulk is low. This gives grain growth law of the form (Eqn. 9) $\bar{D}_t^3 - \bar{D}_o^3 = Kt$. The role of impurity atoms in solution on boundary mobility is better understood in metals⁸²⁻⁸⁵ where in a value of n between 2.5 and 3 has been observed. However, in ceramics the simultaneous presence of aleoalent impurities gives a defect structure which makes interpretation of n and Q_G difficult.

In certain cases⁷⁸ impurities give second phase at the grain boundary even when impurity level is far below the equilibrium solubility limit. The grain growth will then be controlled by second phase coalescence rather than impurity drag. From the expression of M_b (Eqn. 37) in presence of solute impurities it appears that there are two rate controlling mechanisms; the segregation of impurity in the distorted lattice at grain boundary and the diffusion of impurity atom at the grain boundary.

3. Solid Solution Impurities (aleovalent)

Solute impurities with valence different^{86, 87} from that of the host ion affect the defect chemistry of the matrix (which directly controls lattice diffusion), giving anomalously high activation energies for sintering and creep in refractory oxides. It is expected that even for grain boundary migration in oxides doped with aleovalent impurities the activation energies would be significantly different from those observed from tracer diffusion studies in these systems. It has been suggested⁸⁷⁻⁸⁹ that these extrinsic activation energies correspond to vacancy motion and may include in certain cases, terms related to defect creation and the partial heat of solution (endothermic).

The activation energy for boundary migration in presence of aleovalent solute impurity is given by⁸⁷

$$Q_G = \Delta H^m + aH^I + b \Delta H^S + E \quad (38)$$

and represents the sum of the vacancy migration, vacancy creation, impurity solution and, strain energy terms (usually small compared to other terms). The relative contribution of each term to Q_G may not be simple but is expected to depend, among other things, on impurity concentration relative to its solubility limit and the sintering atmosphere. a and b are constants for a given system.

Very small number of foreign ions in the lattice create vacancies whose concentration may be many orders of magnitude greater than that of thermal vacancies. For MgO ⁹⁰ at 1200°C (half of the melting point), the fraction of vacant cation sites can increase from 10^{-8} (intrinsic) to 10^{-6} (extrinsic) by addition of either 0.5 ppm Ti^{4+} or 1 ppm F^- . Anion vacancies⁹¹ can be produced by substituting Li^{1+} for Mg^{2+} .

For soluble fixed aleovalent cation impurities (eg Cr^{3+} in MgO and Mg^{2+} in Al_2O_3), Eq. (38) reduces to

$$Q_G = \Delta H^m \quad (39)$$

Thus, in well defined extrinsic systems the activation energy would be expected to correspond to defect motion alone.

For soluble impurities of variable valence (e.g. Fe^{2+} , Fe^{3+} and Ti^{3+} in Al_2O_3 ^{92, 93} and MgO ⁹⁴), Eqn. (38) becomes

$$Q_G = \Delta H^m + a \Delta H^I \quad (40)$$

and for impurities of invariant valence in a two phase system (e.g. MgO in Al_2O_3 ^{51, 95, 96} wherein concentration of Mg^{2+} exceeds solubility limit giving precipitation).

$$Q_G = \Delta H^m + b \Delta H^S \quad (41)$$

Finally, the important role of sintering atmosphere (oxidizing vs reducing) should be emphasized in determining the type of defect structure in cases like Fe -, Ti -, and Mn - doped Al_2O_3 . Precipitation effects (Eqn. 41) are sensitive to atmosphere as seen for Ti-doped Al_2O_3 ⁹², wherein a reducing atmosphere gives higher concentration of Ti^{3+} , which is more soluble in the matrix than Ti^{4+} .

4. Liquid Phase Impurities

Grain Growth process is observed to accelerate in presence of impurities which form a continuous liquid film^{65, 97} at grain boundaries, that is it wets the grain boundary ($\gamma > 2\gamma_{\ell}$). According to Greenwood⁹⁸, growth of round particles (grains) in a liquid phase involves solution of the smaller grains and growth of the larger, with material transfer being by diffusion in the liquid phase. The solubility (S_R) at the surface of a solid particle of radius R in a liquid, is given by $S_R \propto 1/R$. This can be compared to evaporation at the surface of a solid particle (radius R) which is directly related to the equilibrium vapor pressure which in turn is inversely proportional to R. The driving force for the increase in average particle size of a solid phase dispersed in a liquid phase is the consequent reduction in surface area. The process occurs in three steps: (1) dissolving of a grain (2) material transport by diffusion through the liquid phase, and (3) precipitation on the growing grain. The amount of liquid needed for liquid phase-influenced grain growth is very small.

Several authors^{99, 100, 101} have noted that the rate controlling process during coalescence is the surface reaction at the liquid-solid interface. (They observed activation energies higher than that expected if diffusion in a liquid phase is rate controlling.) This case yields a growth law $\bar{D}_t^2 \propto t$ which also holds for solid state grain growth involving movement of ions across an interface. (See Eqn. 7). Others^{47, 102} have shown that the rate of densification in a system containing a liquid phase is controlled by diffusion of ions through the liquid phase and it has been suggested that such diffusion is also limiting for grain growth^{97, 103, 104} in presence of a liquid phase. The driving force for diffusion in liquid phase is the concentration gradient of the diffusing species in the liquid.

The derivation⁹⁷ of growth law in presence of liquid phase assumes implicitly that the distribution of liquid within the two phase mixture is not a function of grain size. For a constant diffusion coefficient, a thin liquid layer, and a constant volume fraction of liquid, the concentration gradient is inversely proportional to the average thickness of the liquid layer (δ_l). Since $\delta_l \propto \bar{D}_t$, δ_l increases with time and grain growth rate diminishes.

The final expression for grain growth in presence of liquid second phase is given⁹⁷ by

$$\bar{D}_t^3 = \frac{6D_l S M \gamma_l}{\rho^2 RT} t \quad (42)$$

This cubic growth law ($n = 3$) was observed by Bruist et al.¹⁰⁴, Lay⁹⁷ and Nicholson¹⁰³, and the growth rate depended on amount of liquid phase present. Lay⁹⁷ observed absolute growth rate increased as amount of liquid decreased. On the other hand at constant temperature, Nicholson¹⁰³ observed an increase in rate constant with amount of the liquid phase owing to the larger area of solid-liquid interface. Also, the growth rate depends¹⁰⁵ on magnitude of the dihedral angle (Φ) between grains that share common grain boundaries. It is observed¹⁰⁴⁻¹⁰⁶ that the growth rate decreases with an increase in the dihedral angle (Φ)

which is due to either (1) its influence on the curvature of solid-liquid interfaces which controls the solution-precipitation rates or (2) the fraction of grain surface in contact with the liquid phase decreases. Further, ϕ depends on the degree of impurity segregation at the grain boundary; MgO segregates at grain boundaries of Al_2O_3 (thus lowering the surface tension) giving $\phi = 40^\circ$, while $\phi = 10^\circ$ for CaO and SiO_2 which segregate to a lesser extent. As a result grain growth observed for MgO mixture is slower than in the other two.

5. Summary of Grain Growth in Presence of Impurities

Grain growth kinetics is influenced by presence of porosity and impurities. When grain growth is not controlled by porosity, it depends on grain boundary mobility which is only controlled by impurities by any of the processes mentioned in previous section. On the other hand, for porosity-controlled boundary migration, impurities indirectly play a role in promoting pore transport (volatile specie helps vapor transport while solute impurities may influence solid-state diffusion). Also, impurities in some cases, may aid densification, for example, by formation of a liquid phase, or acting as "carrier" agents for molecules of the less volatile matrix.

C. Generalized Expression for Inhibited Grain Growth

To summarize the various aspects of grain boundary migration discussed above, one can integrate all the information and formulate a generalized equation for boundary migration. Since one experimentally studies \bar{D}_t , rather than $\frac{d\bar{D}}{dt}$, as a function of sintering time (t), Eqn. (9) (instead of Eqn. (4)) will be rewritten with special emphasis on the factors and their material dependences which control them in a given situation.

$$\bar{D}_t^n - \bar{D}_o^n = tB \gamma (\beta, \theta) a \exp \frac{\Delta S_G^{(V_a)}}{R} \exp - \left(Q_G^i(X, v, T, atm) + Q_G^p + Q_G^l(c) \right) / RT \quad (43)$$

where B is a constant independent of material parameters.

and (1) $n = 2 + p + i$. $p = i = 0$ for normal (unhibited) grain growth. In presence of interconnected porosity n is, in some cases, observed to be 2 but probably by a different mechanism. Sec. IV-A-5. For pore control (< 5% porosity), $i = 0$ and $p = 0, 1, 2$ depending on mode of pore transport and pore location (Table III). For impurity control, $p = 0$ and $i = 1$ for most cases as discussed in Sec. IV-B. (2) γ depends on nature of second phase (β) at grain boundary. If wetting by second phase is evident, then γ decreases. For liquid phase γ is energy of solid-liquid interface. γ is expected to increase with misorientation (θ) between grains in absence of second phase at grain boundary. The dependence on temperature is slight and hence not introduced. (3) The dependence of lattice parameter, a , on temperature and solute segregation at grain boundary is a second order effect and hence not very important. (4) ΔS_G is related to volume of the activated complex,¹⁰⁷ a measure of this quantity should be volume (V_a) of the diffusing specie. (5) Q_G is separated into Q_G^i , Q_G^p and Q_G^l depending on whether impurity, pore or liquid phase controls boundary migration. Each of these terms are further discussed below. It is expected that at a given time only one of these will be rate controlling.

a) The impurity can be either in solid solution and/or as second phase

$$Q_G^i = Q_1 + Q_2$$

Q_1 = intrinsic activation energy of the diffusing specie, either in the lattice or along the grain boundary. For second phase impurity, the rate determining mechanism is coarsening of second phase particles and Q_1 = lattice diffusion of the impurity.

Q_2 (correction term) = 0 at high temperature, low impurity content
or when $\Delta v = 0$ (intrinsic behavior)
= negative if aliovalent impurities ($\Delta v \neq 0$)
with fixed valence present and corresponds to

- activation energy for vacancy formation (extrinsic behavior). Also ^{66b} negative for hyperstoichiometric UO_2 (atmosphere slightly oxidizing).
- = positive if aleovalent impurities ($\Delta v \neq 0$) have variable valence depending on the sintering atmosphere (e. g. partial pressure of oxygen) or if concentration of impurity exceeds the solubility limit (X).
- b) Q_G^p = Activation energy in presence of porosity controlled grain growth and depends on mechanism of pore transport i. e. it could correspond to lattice or surface diffusion or heat of vaporization if vapor transport is rate controlling. If interconnected porosity is present, the rate of pore removal is controlling and activation energy corresponds to lattice diffusion of the cation, in most cases.
- c) Q_G^l = Activation energy for diffusion of the rate controlling specie in the liquid phase at the grain boundary. It depends on the concentration(c) of the liquid phase which is sensitive to temperature, which means Q_G^l has a slight temperature dependence.

V. Conclusions

(1) In the generalized expression, it is not anticipated that all terms and their dependences could ever be completely defined in a single experimental situation; rather the usefulness of the expression lies in relating changes in experimentally observed behavior to changes in individual terms in the expression and the physical factors predicting such changes.

(2) Grain boundary migration is a complex phenomenon not yet understood in terms of rate controlling mechanisms which change with time and experimental conditions like firing temperature^{67c} and furnace atmosphere.⁶³ Impurities are known to control grain growth but their interaction with the matrix in relation to location and defect chemistry is not at all well defined.

(3) Extensive research is needed to interpret the experimental activation energies in terms of the nature of the diffusing specie (cation, anion or a impurity-vacancy complex) and the type of diffusion involved, e. g. intergranular, intragranular or vapor transport.

(4) Various experimental studies on a particular system often show discrepancies in observed behavior which cannot be explained by a difference in thermal conditions alone. This clearly indicates that there are still some variable material parameters which have been overlooked and a thorough analysis should take into account factors like thermal history (vacancy concentration), state of stress (dislocation density) and exact impurity levels. These factors are known to affect mechanical behavior¹⁰⁸⁻¹¹⁰ in ceramics and it is expected that grain growth should be sensitive to them also.

(5) Hence the analysis of experimental grain growth data must be based on specimen history and microstructural observations. A direct comparison with established theories may not always show complete agreement, primarily because the individual conditions prevalent in a real system may be beyond the scope of a theoretical model. For

example, grain growth in presence of a liquid phase follows $n = 3$ kinetics by theory (Sec.IV-B-4). However, a value of $n = 4$ has been reported in certain cases¹¹¹⁻¹¹³ suggesting that surface diffusion¹¹⁴ is favorable in these systems. This should be interpreted in light of the presence of conditions (e. g. defect structure) promoting surface diffusion and not indicative of a typical behavior in presence of a liquid phase.

(6) This discussion is in general also applicable both to metals and powder metallurgy components. However, the role of impurities in relation to grain boundaries is more specific to ceramics and revised interpretation should be included for metals.

References

1. F. P. Knudsen, "Dependence of Mechanical Strength of Brittle Polycrystalline Specimens on Porosity and Grain Size," J. Am. Ceram. Soc., 42 [8] 376-87 (1959).
2. R. M. Spriggs, T. Vasilos, and L. A. Brissette, "Grain Size Effects in Polycrystalline Ceramics," Chapter 20 in Materials Science Research, vol. 3. The Role of Grain Boundaries and Surfaces in Ceramics. Edited by W. W. Kriegel and H. Palmour, III, Plenum Press, 1966.
3. T. Vasilos, J. B. Mitchell and R. M. Spriggs, "Mechanical Properties of Pure, Dense, Magnesium Oxide as a Function of Temperature and Grain Size," J. Am. Ceram. Soc., 47 [12] 606-10 (1964).
4. R. M. Spriggs and T. Vasilos, "Effect of Grain Size on the Transverse Bend Strength of (Hot-pressed) Alumina and Magnesia," J. Am. Ceram. Soc., 46[5] 224-28 (1963).
5. a. R. L. Coble, pp 213-228 in Ceramic Fabrication Processes. Edited by W. D. Kingery. Technology Press of Massachusetts Institute of Technology, Cambridge, and John Wiley & Sons, Inc., New York, 1960.
b. George Economos, "Effect of Microstructure on the Electrical and Magnetic Properties of Ceramics," ibid , pp 201-213.
6. Alan Arias, "Investigation of Thermal Shock Resistance of Zirconia with Metal Additions," NASA TND-2464, 72 pp., September 1964.
7. T. D. McGee, "Grain Boundaries in Ceramic Materials," pp 3-32 in Materials Science Research, vol. 2. Edited by H. Otte and S. Locke. Plenum Press, New York 1965.
8. R. Hanna, "Infrared Properties of Magnesium Oxide," J. Am. Ceram. Soc., 48 [7] 376-380 (1965).
9. P. G. Shewmon, "Transformation in Metals," Chapt. 3, McGraw-Hill Book Company, New York, 1969.
10. David Turnbull, "Theory of Grain Boundary Migration Rates," Trans. A.I.M.E. 191, 661-665 (1951).

11.
 - a. J. E. Burke and D. Turnbull, "Recrystallization and Grain Growth," *Progr. Metal. Phys.*, 3, 220-92, Pergamon Press, Ltd., London, 1952. 334 pp.
 - b. J. E. Burke, "The Fundamentals of Recrystallization and Grain Growth," pp 1-73 in *Grain Control in Industrial Metallurgy*. American Society for Metals, Cleveland, Ohio (1949).
 - c. J. E. Burke, "Grain Growth in Ceramics," Chapter 16, pp. 109-16 in *Kinetics of High Temperature Processes*. Edited by W. D. Kingery. Technology Press of Massachusetts Institute of Technology, Cambridge and John Wiley & Sons, Inc., New York, 1959. 326 pp.
12. P. Feltham, "Grain Growth in Metals," *Acta Met.*, 5[2] 97-105 (1957).
13. M. Hillert, "On the Theory of Normal and Abnormal Grain Growth," *ibid.*, 13 [3] 227-38 (1965).
14. H. Hu and B. B. Rath, "On the Time Exponent in Isothermal Grain Growth," *Metallurgical Transactions*, 1 [11], 3181-84 (1970).
15. P. Gordon and R. A. Vandermeer, "Grain Boundary Migration." Chapter 6 in *Recrystallization, Grain Growth and Textures*. Edited by H. Margolin, Amer. Soc. of Metals, Cleveland, Ohio (1966).
16. G. F. Bolling and W. C. Winegard, "Grain Growth in Zone-Refined Lead," *Acta Met.*, 6 [4] 283-87 (1958).
17.
 - a. E. L. Holmes and W. C. Winegard, "Grain Growth in Zone-Refined Tin," *Acta Met.*, 7 [6] 411-14 (1959).
 - b. E. L. Holmes and W. C. Winegard, "The Effect of Pb and Bi on Grain Growth in Zone-Refined Sn," *Trans. TMS-AIME*, 224 [4] 945-49 (1962).
18. R. M. Spriggs, L. A. Brisette and T. Vasilos, "Grain Growth in Fully Dense Magnesia," *J. Amer. Ceram. Soc.*, 47 [8] 417-18 (1964).
19.
 - a. P. A. Beck, J. C. Kremer, L. J. Demer, and M. L. Holzworth, "Grain Growth in High-Purity Aluminum and in an Aluminum-Magnesium Alloy," *Trans. AIME*, 175, 372-94 (1948).
 - b. P. A. Beck, J. Towers, Jr., and W. D. Manly, "Grain Growth in 70-30 Brass." *ibid.*, 175, 162-168 (1948).

20. R. L. Fullman, Metal Interface, p. 179, Amer. Soc. Met., Cleveland, Ohio (1952).
21. J. P. Nielsen, "Recrystallization, Grain Growth and Textures," p. 286. Edited by H. Margolin, Amer. Soc. of Metals, Cleveland, Ohio (1966).
22. J. W. Cahn, "Impurity-Drag Effect in Grain Boundary Motion," Acta Met., 10 [9] 789-98 (1962).
23. K. Lucke and K. Detert, "Quantitative Theory of Grain-Boundary Motion and Recrystallization in Metals in Presence of Impurities," Acta Met., 5 [1] 628-37 (1957).
24. E. S. Machlin, "Theory of Solute-Atom-Limited Grain Boundary Migration," Trans. AIME, 224 [11] 1153-67 (1962).
25. P. J. Jorgensen and J. H. Westbrook, "Role of Solute Segregation at Grain Boundaries During Final Stage Sintering of Al_2O_3 ," J. Am. Ceram. Soc., 47 [7] 332-38 (1964).
26. R. E. Reed-Hill, Chapter 7 in Physical Metallurgy Principles. D. Van Nostrand Company, Inc., New York, 1964.

27. P. A. Beck, P. R. Speery and H. Hu, "The Orientation Dependence of the Rate of Grain Boundary Migration," J. Appl. Phys. 21 [5] 420-425 (1950).
28. R. L. Coble, "Sintering Crystalline Solids. I. Intermediate and Final State Diffusion Models," *ibid.*, 32 [5] 787-92 (1961).
29. F. A. Nichols, "Further Comments on the Theory of Grain Growth in Porous Compacts," J. Am. Ceram. Soc., 51 [8] 468-69 (1968).
30. F. A. Nichols, "Kinetics of Diffusional Motion of Pores in Solids, A Review," J. Nucl. Mat. 30 [1,2] 143-65 (1969).
31. a. W. D. Kingery and B. Francois, "Grain Growth in Porous Compacts," J. Am. Ceram. Soc., 48 [10] 546-47 (1965).
b. W. D. Kingery and B. Francois, "The Sintering of Crystalline Oxides, I. Interactions between Grain Boundaries and Pores." pp 471-98 in Sintering and Related Phenomena. Edited by G. C. Kuczynski, N. A. Hooton and C. F. Gibbon. Gordon and Breach, Science Publishers, New York, 1967.
32. R. W. Rice, "The Effect of Gaseous Impurities on the Hot Pressing and Behaviour of MgO, CaO and Al₂O₃," Proc. Brit. Ceram. Soc. 12 [3] 99-123 (1969).
33. M. H. Leipold and C. M. Kapadia, "Effect of Anions on Hot Pressing of MgO," J. Am. Ceram. Soc., 56[4] 200-203 (1973).
34. R. S. Gordon, D. D. Marchant, and G. W. Hollenberg, "Effect of Small Amounts of Porosity on Grain Growth in Hot-Pressed Magnesium Oxide and Magnesiowastite," *ibid.*, 53 [7] 399-406 (1970).
35. T. K. Gupta, "Kinetics and Mechanisms of Pore Growth in MgO," J. Mater. Sci., 6 [7] 989-997 (1971).
36. R. J. Brook, "Pores and Grain Growth Kinetics," J. Amer. Ceram. Soc., 52 [6] 339-340 (1969).
37. F. A. Nichols, "Theory of Grain Growth in Porous Compacts," J. Appl. Phys. 37 [13] 4599-4602 (1966).

38. C. M. Kapadia and M. H. Leipold, "Correlation of Pore Size and Grain Size During Grain Growth of Oxides," J. Amer. Ceram. Soc. 56 [5] 289 (1973).
39. P. G. Shewmon, "The Movement of Small Inclusions in Solids by a Temperature Gradient," Trans. AIME 230 [5] 1134-1137 (1964).
40. M. J. Bannister, "Kinetics of Sintering and Grain Growth of Beryllia," J. Nucl. Mat. vol. 14, 315-321 (1964).
41. C. M. Kapadia, "Grain Boundary Mobility in Anion Doped MgO." Ph.D. Thesis. To be published.
42. a. J. R. MacEwan, "Grain Growth in Sintered Uranium Dioxide: 1, Equiaxed Grain Growth," J. Amer. Ceram. Soc., 45[1] 37-41 (1962).
b. J. R. MacEwan and J. Hayashi, "Grain Growth in UO_2 .III. Some Factors Influencing Equiaxed Grain Growth," Proc. of Brit. Ceram. Soc. No. 7, 245-271 (1967).
43. R. L. Coble, "Sintering Crystalline Solids. II. Experimental Test of Diffusion Models in Powder Compacts," J. Appl. Phys. 32 [5] 793-799 (1961).
44. J. White, "Magnesia-Based Refractories," Chapter 2 in High Temperature Oxides, Part I," Edited by Allen M. Alper. Academic Press, New York, 1970.
45. J. L. Woolfrey, "Feasibility of Dispersed Phase Grain Refinements in Ceramics," AAEC/E170 (February 1967).
46. R. C. Lowrie, Jr., and I. B. Cutler, "The Effect of Porosity on the Rate of Grain Growth of Magnesia," pp 527-539 in Reference 31b.
47. R. A. Brown, "Sintering in Very Pure Magnesium Oxide and Magnesium Oxide Containing Vanadium," Am. Ceram. Soc. Bull., 44 [6] 483-487 (1965).
48. J. Von Neumann, in discussion of C. S. Smith's "Grain Shapes and Other Metallurgical Applications of Topology," pp 65-110 in Metal Interfaces. American Society for Metals, Cleveland, Ohio 1952.

49. J. E. Burke, "Sintering and Microstructure Control," General Electric Company Rept., 68-C-368 (1968).
50. P. J. Jorgensen, "Modification of Sintering Kinetics by Solute Segregation in Al_2O_3 ," J. Am. Ceram. Soc., 48 [4], 207 (1965).
51. C. A. Bruch, "Sintering Kinetics for the High Density Alumina Process," Am. Ceram. Soc. Bull., 41 [12] 799-806 (1962).
52. P. J. Jorgensen and R. C. Anderson, "Grain Boundary Segregation and Final Stage Sintering of Y_2O_3 ," J. Am. Ceram. Soc. 50 [11], 553-558 (1967).
53. R. J. Brooks, "Pore-Grain Boundary Interactions and Grain Growth," *ibid.*, 52 [1] 56-57 (1969).
54. a. K. Langrod, "Graphite as Grain Growth Inhibitor in Hot-Pressed Beryllium Oxide," *ibid.*, 48 [2], 110-111 (1965).
b. E. C. Duderstadt and J. E. White, "Sintering BeO to Variable Densities and Grain Sizes," Am. Ceram. Soc. Bull. 44 [11] 907-911 (1965).
c. E. Clougherty, D. Kalish and E. T. Peters, "Research and Development of Oxidation Resistant Diborides," Air Force Materials Laboratory Rept. AFML-TR-68-190.
55. M. J. Bannister, "Interdependence of Pore Removal and Grain Growth During Later Stages of Sintering in Beryllium Oxide," pp 581-603 in Reference 31b.
56. T. K. Gupta, "Possible Correlation Between Density and Grain Size During Sintering," J. Am. Ceram. Soc., 55 [5] 276-277 (1972).
57. T. K. Gupta and R. L. Coble, "Sintering of ZnO :I," *ibid.*, 51 [9] 521-525 (1968).
58. T. E. Clare, "Sintering Kinetics of Beryllia," *ibid.*, 49 [3] 159-165 (1966).
59. R. L. Coble and T. K. Gupta; "Intermediate Stage Sintering," pp 423-444 in Reference 31b.

60. S. Samanta and R. L. Coble, "Correlation of Grain Size and Density During Intermediate Stage Sintering of Ag," J. Amer. Ceram Soc. 55 [11] 583 (1972).
61. A. U. Daniels, Jr., R. C. Lowrie, Jr., R. L. Gibby and I. B. Cutler, "Observations on Normal Grain Growth of Magnesia and Calcia," *ibid.*, 45 [6] 282-85 (1962).
62. T. K. Gupta, "Sintering of MgO: Densification and Grain Growth," J. Mater. Sci., 6 [1] 25-32 (1971).
63. Yoshio Iida, "Sintering of High-Purity Nickel Oxide," Jn. Am. Ceram. Soc. 41 [10] 397-406 (1958).
64. I. Amato, R. L. Colombo, A. Petruccioli Balzari, "Grain Growth in Pure and Titania-Doped Uranium Dioxide," J. Nucl. Mater. 18 [3] 252-260 (1966).
65. E. J. Felten, "Sintering Behavior of Beryllium Oxide," J. Amer. Ceram. Soc., 44 [6] 251-255 (1961).
66. a. J. Belle, "Properties of Uranium Dioxide in Fuel Elements Conference, AEC Report TID-7546 (1958).
- b. I. Amato, R. L. Colombo and A. M. Protti, "Influence of Stoichiometry on the Rate of Grain Growth of UO_2 ," J. Am. Ceram Soc., 46 [8] 407 (1963).
- c. A. M. Ross and G. L. Whitton, AECL Report 1563, CFRD-1100 (1962).
- d. H. Stehle, Paper presented at joint meeting of Deutsche Gesellschaft f. Metallkunde and the Deutsche Keramische Gesellschaft on "Keramische Werkstoffe in Reaktorbau," Baden-Baden, West Germany (1962).
- e. H. H. Hausner, USAEC Report GEAP-4315 U963.
67. a. T. Y. Tien and E. C. Subbarao, "Grain Growth in $\text{Ca}_{0.16}\text{Zr}_{0.84}\text{O}_{1.84}$," J. Amer. Ceram. Soc., 46 [10] 489-492 (1963).

67. b. T. Yamaguchi, "Effect of Powder Parameters on Grain Growth in Manganese-Zinc Ferrite", J. Am. Ceram. Soc., 47 [3] 131-133 (1964).
- c. P. Levesque, L. Gerlech, and J. Zneimer, "Grain Growth in Nickel Ferrites," *ibid.*, 41 [8] 300-303 (1958).
68. E. A. Aitken, "Sintering Kinetics of Tungsten Trioxide," pp 793-805 in Reference 31b.
69. G. C. Nicholson, "Grain Growth in Zinc Oxide," J. Amer. Ceram. Soc. 48 [4] 214-15 (1965).
70. a. S. B. Austerman, "Diffusion of Be in BeO," NAA-SR-3170 (Dec. 1958). 'Part II', NAA-SR-5893 (May 1, 1961).
- b. H. J. DeBruin and G. M. Watson, "Self Diffusion of Beryllium in Unirradiated Beryllium Oxide," J. Nucl. Mater. vol. 14, 239-247 (1964).
- c. A. E. Paladino and W. D. Kingery, "Aluminum Ion Diffusion in Aluminum Oxide," J. Amer. Ceram. Soc., 37 [5] 957-962 (1962).
- d. R. Linder and G. Parfitt, "Diffusion of Radioactive Magnesium in Magnesium Oxide Crystals," J. Chem. Phys. 26 [1] 182-185 (1957).
- e. R. Linder, "Diffusion of Calcium in Calcium Oxide," Acta Chem. Scand. 6 [4] 468 (1952).
- f. Y. P. Gupta and L. J. Weirick, "Self Diffusion of Calcium in Single Crystal Calcium Oxide," J. Phys. Chem. Solids 28 [5] 811-821 (1967).
- g. R. Linder, "Diffusion of Radioactive Zinc in Zinc-Iron Spinel and Zinc Oxide," Acta Chem. Scand., 6 [4] 457-467 (1952) (in German).
- h. J. S. Choi and W. J. Moore, "Diffusion of Nickel in Single Crystals of Nickel Oxide," J. Phys. Chem., 66 [7] 1308-1311 (1962).

70. i. R. Linder and A. Akerstrom, "Diffusion of Nickel-63 in Nickel Oxide (NiO)," Discussions Farad. Soc., 23, 133-36 (1957).
j. H. Matzke, "On Uranium Self-Diffusion in UO_2 and $\text{UO}_2 + x$," J. Nucl. Mater. 30 [1,2] 26-35 (1969).
k. S. Yajima, H. Furuya, T. Hirai, "Lattice and Grain Boundary Diffusion of Uranium in UO_2 ," J. Nucl. Mater. 20[2] 162-70 (1966).
l. A. B. Auskern and J. Bell, "Uranium Ion Self-Diffusion in UO_2 ," J. Nucl. Mater., 3 [3] 311-319 (1961).
m. J. F. Marin and P. Contamin, "Uranium and Oxygen Self-Diffusion in UO_2 ," J. Nucl. Mater. 30 [1,2] 16-25 (1969).
71. a. S. K. Dutta and R. M. Spriggs, "Grain Growth in Fully Dense ZnO," J. Amer. Ceram. Soc. 53 [1] 61-62 (1970).
b. Alan Arias, "Effect of Inclusions on Grain Growth of Oxides," *ibid.*, 49 [11] 621-623 (1966).
72. M. V. Speight, "Growth Kinetics of Grain-Boundary Precipitates," *ibid.*, 16 [1] 133-135 (1968).
73. P. G. Shewmon, Chapter 7 in Reference 9
74. P. A. Beck, M. L. Holzworth, P. Sperry, "Effect of a Dispersed Phase on Grain Growth in Al-Mn Alloys," Trans. AIME, 180, 163-192 (1949).
75. M. F. Ashby and R. M. Centamore, "Measurements of the Dragging Small Oxide Particles by Migrating Grain Boundaries in Copper," Tech. Rept. 518 Division of Engineering and Applied Physics. Harvard University. Cambridge, Massachusetts.
76. W. D. Kingery, "Surfaces and Interfaces," Chapter 7 in Introduction to Ceramics, John Wiley & Sons Inc., New York (1967).
77. a. P. J. Jorgensen and J. H. Westbrook, "Role of Solute Segregation at Grain Boundaries During Final-Stage Sintering of Alumina," J. Am. Ceram. Soc., 47 [7] 332-338 (1964).
b. J. H. Westbrook and K. T. Aust, "Solute Hardening at Interfaces in High-Purity Lead-I Grain and Twin Boundaries," Acta Met., 11 [10] 1151-1163 (1963).

78. M. H. Leipold, "Impurity Distribution in MgO," J. Amer. Ceram. Soc., 49 [9] 498-502 (1966).
79. a. B. J. Wuensch and T. Vasilos, "Grain Boundary Diffusion in MgO," *ibid.*, 47 [2] 63-68 (1964).
b. B. J. Wuensch and T. Vasilos, "Origin of Grain Boundary Diffusion in MgO," *ibid.*, 49 [8] 433-436 (1966).
80. C. Zener, "Relation Between Residual Strain Energy and Elastic Modulus," Acta Cryst., 2, 163-166 (1949).
81. R. J. Brook, "The Impurity-Drag Effect and Grain Growth Kinetics," Scripta Metallurgica, 2 [7] 375-378 (1968).
82. G. F. Bolling and W. C. Winegard, "Some Effects of Impurity on Grain Growth in Zone-Refined Lead," Acta Met., 6 [4] 288-92 (1958).
83. K. T. Aust and J. W. Rutter, "Temperature Dependence of Grain Boundary Migration in High Purity Lead Containing Small Additions of Tin," Trans. Am. Inst. Mining Met. Engrs. 215 [5] 820-831 (1959).
84. J. W. Rutter and K. T. Aust, "Kinetics of Grain-Boundary Migration in High Purity Lead Containing Very Small Additions of Silver and Gold," *ibid.*, 218 [8] 682-688 (1960).
85. P. Gordon and R. A. Vandermeer, "The Mechanism of Boundary Migration in Recrystallization," Trans. AIME, 224 [9] 917-928 (1962).
86. John T. Jones, Pranab Maitra, and Ivan B. Cutler, "Role of Structural Defects in the Sintering of Alumina and Magnesia," J. Am. Ceram. Soc., 41 [9] 353-357 (1958).
87. G. W. Hollenberg and R. S. Gordon, "Origin of Anomalously High Activation Energies in Sintering and Creep of Impure Refractory Oxides," *ibid.*, 56 [2] 109-110 (1973).
88. R. J. Brook, "Effect of TiO_2 on the Initial Sintering of Al_2O_3 ," *ibid.*, 55 [2] 114-115 (1972).
89. S. K. Roy and R. L. Coble, "Solubilities of Magnesia, Titania, and Magnesium Titanate in Aluminum Oxide," *ibid.*, 51 [1] 1-6 (1968).

90. I. B. Cutler, "Sintered Alumina and Magnesia," Chapter 3 in High Temperature Oxides Part III, edited by Allen Alper. Academic Press, New York 1970.
91. L. M. Atlas, "Effect of Some Lithium Compounds on Sintering of MgO," J. Am. Ceram. Soc., 40 [6]196-199 (1957).
92. G. W. Hollenberg and R. S. Gordon, "Effect of Oxygen Partial Pressure on the Creep of Poly crystalline Al_2O_3 Doped with Cr, Fe, or Ti," *ibid.*, 56 [3] 140-147 (1973).
93. R. D. Bagley, I. B. Cutler and D. L. Johnson, "Effect of TiO_2 on Initial Sintering of Al_2O_3 ," *ibid.*, 53 [3] 136-141 (1970).
94. G. C. Nicholson, "Grain Growth in Magnesium Oxide Containing Iron Oxide or Titanium Dioxide," *ibid.*, 49 [1] 47-49 (1966).
95. Alain Mocellin and W. D. Kingery, "Creep Deformation in MgO-Saturated Large-Grain-Size Al_2O_3 ," *ibid.*, 54 [7] 339-341 (1971).
96. D. L. Johnson and I. B. Cutler, "Diffusion Sintering: I," *ibid.*, 46 [11] 541-545 (1963); "II," *ibid.*, pp 545-550.
97. K. W. Lay, "Grain Growth in $UO_2-Al_2O_3$ in the Presence of a Liquid Phase," *ibid.*, 51 [7] 373-376 (1968).
98. G. W. Greenwood, "Growth of Dispersed Precipitates in Solutions," *Acta Met.*, 4 [3] 243-248 (1956).
99. L. Skolnick; pp 92-97 in Reference 11c.
100. Carl Wagner, "Theory of Precipitate Change by Redissolution," *Z. Elektrochem.*, 65 [7-8] 581-591 (1961).
101. L. H. VanVlack and O. Riegger, "Microstructures of Magnesiowustite $[(Mg, Fe)O]$ in the Presence of SiO_2 ," *Trans. AIME*, 224 [5] 957-965 (1962).
102. a. W. D. Kingery, "Densification During Sintering in the Presence of a Liquid Phase: I," *J. Appl. Phys.*, 30 [3]301-306 (1959); 'II', *ibid.*, 307-310.
b. W. D. Kingery, E. Niki and M. Narasimhan, "Sintering of Oxide and Carbide-Metal Compositions in Presence of a Liquid Phase," *J. Am. Ceram. Soc.*, 44 [1] 29-35 (1961).

103. G. C. Nicholson, "Grain Growth in Magnesium Oxide Containing a Liquid Phase," *ibid.*, 48 [10] 525-528 (1965).
104. D. S. Buist, B. Jackson, I. M. Stephenson, W. F. Ford and J. White, "Kinetics of Grain Growth in Two-Phase (Solid-Liquid) Systems," *Trans. Brit. Ceram. Soc.*, 64 [4] 173-209 (1965).
105. J. White, "Factors Affecting the Kinetics of Grain Growth and Densification in Ceramic Bodies Containing a Liquid Phase. *Materials Science Research*, vol. 4, pp. 96-120, Plenum Press, New York (1969).
106. B. Jackson, W. F. Ford and J. White, *Trans.-Brit. Ceram Soc.* 62, 577 (1963).
107. B. J. Wuensch and T. Vasilos, "Diffusion of Transition Metal Ions in Single-Crystal MgO," *J. Chem. Phys.*, 36[11] 2917-2922 (1962).
108. R. J. Stokes, "Thermal-Mechanical History and the Strength of Magnesium Oxide Single Crystals: I," *J. Am. Ceram. Soc.*, 48 [2] 60-67 (1965). "II, Etch Pit and Electron Transmission Studies," *ibid.*, 49 [1] 39-46 (1966).
109. J. Rasmussen, G. Stringfellow, I. Cutler and S. Brown, "Effect of Impurities on the Strength of Poly crystalline Magnesia and Alumina," *ibid.*, 48 [3] 146-150 (1965).
110. J. B. Wachtman, Jr., "Mechanical Properties of Ceramics: An Introductory Survey," *Amer. Ceram. Soc. Bull.* 46 [8] 756-772 (1967).
111. J. T. Smith and C. W. Spencer, "Grain Growth in the Presence of an Intergranular Liquid," *Trans. AIME*, vol. 227, 783-784 (1963).
112. R. H. Krock, Presented at Fifth Plansee Seminar, June 22, 1964, Reutte/Tyrol, Austria.
113. Y. Okamoto, *Journal of Japanese Soc. Powder Metallurgy*, 9, 4 (1962).
114. C. Herring, "Effect of Change of Scale on Sintering Phenomena," *J. App. Physics* 21 [4] 301-303 (1950).